catalysts

MDPI

Article

Highly Dispersed PdNPs/α-Al_2O_3 Catalyst for the Selective Hydrogenation of Acetylene Prepared with Monodispersed Pd Nanoparticles

Huoli Zhang [1], Youchao Wang [1,*], Yan Wang [2], Jianliang Cao [1], Peng Kang [3], Qingjie Tang [1] and Mingjie Ma [1]

1 School of Chemistry and Chemical Engineering, Henan Polytechnic University, Jiaozuo 454000, China; zhanghuoli@hpu.edu.cn (H.Z.); caojianliang@hpu.edu.cn (J.C.); tangqj521@163.com (Q.T.); mingjie8@163.com (M.M.)

2 State Key Laboratory Cultivation Base for Gas Geology and Gas Control, Henan Polytechnic University, Jiaozuo 454000, China; yanwang@hpu.edu.cn

3 Sinopec Beijing Research Institute of Chemical Industry, Beijing 100013, China; kangpeng.bjhy@sinopec.com

* Correspondence: wangyouchao@hpu.edu.cn; Tel.: +86-391-398-7440

Academic Editors: Tian-Yi Ma, Jian-Rong (Jeff) Li and Cláudia Gomes Silva
Received: 28 March 2017; Accepted: 25 April 2017; Published: 28 April 2017

Abstract: Pd nanoparticles (PdNPs) stabilized by methyl cellulose (MC) were synthesized in an aqueous solution, which are monodispersed nanoparticles. PdNPs/α-Al_2O_3 catalyst was prepared with monodispersed PdNPs and showed better catalytic performance than Pd/α-Al_2O_3 catalyst prepared by the incipient wetness impregnation method using $Pd(NO_3)_2$ as a precursor. The catalysts were characterized by transmission electron microscopy (TEM), scanning electron microscopy (SEM), energy dispersive X-ray spectroscopy (EDS), X-ray photoelectron spectroscopy (XPS), X-ray powder diffraction (XRD) and inductively coupled plasma mass spectrometry (ICP-MS). It was found that monodispersed PdNPs were spherical or elliptical nanoparticles with exposed (111) and (100) facets, and the PdNPs/α-Al_2O_3 catalyst showed a more concentrated distribution of Pd particles on the surface of α-Al_2O_3 support than the Pd/α-Al_2O_3 catalyst. The preparation method achieved the highly dispersed PdNPs/α-Al_2O_3 catalyst with smaller Pd particle size and decreased the aggregation of Pd active sites, which was responsible for higher acetylene conversion and ethylene selectivity.

Keywords: monodispersed Pd nanoparticles; acetylene conversion; selective hydrogenation; α-Al_2O_3 support; heterogeneous catalysis

1. Introduction

Industrially, ethylene is an important chemical for polymerization to polyethylene. However, ethylene-rich feed stream contains trace amount of acetylene (0.5–2% by volume) for the tail-end hydrogenation reactor. The small trace of acetylene as impurity has to be reduced to less than 5 ppm [1–3]. For the selective hydrogenation of acetylene, supported Pd catalysts are used for the catalytic removal process. Therefore, supported Pd catalysts with low Pd loading still have attracted much attention in recent years [4–10]. The recent advance on supported Pd catalysts is to increase their ethylene selectivity and enhance their long-term stability. For improving the performance of supported Pd catalysts, bimetallic Pd catalysts have been investigated extensively with the addition of a second metal as a promoter to dilute Pd ensemble size [11–22].

For monometallic Pd catalysts, the shape and size of Pd nanoparticles (PdNPs) are very important for Pd catalysts such as core–shell Pd nanocatalysts, magnetic Pd catalysts, porous carbon nanocomposite Pd catalysts and so on, which also have attracted much attention in the last few

years [23,24]. For the selective hydrogenation of acetylene, Yarulin et al. [25] investigated the structure sensitivity of acetylene hydrogenation on catalysts with controlled shape of PdNPs by a colloidal method using (polyvinyl pyrrolidone) PVP as the stabilizer. The result shows that the shape of PdNPs does not affect the catalyst selectivity, but the activity decreases in the order Pdoct > Pdco > Pdcub. Crespo-Quesada et al. [26] also prepared Pd nanocubes using PVP as the stabilizer and investigated the effect of stabilizer removal and catalytic performance. In addition, He et al. [27] reported that supported Pd nanowire and cuboctahedron catalysts were synthesized in an ethylene glycol-poly (vinylpyrrolidone)-KBr system using a precipitation-reduction method. The activities of the Pd nanowire catalysts were significantly higher than those of the cuboctahedron catalysts owing to the exposure of larger numbers of Pd atoms, which resulted in excessive hydrogenation and a decrease in ethylene selectivity. Kim et al. [28] reported that cubic PdNPs were synthesized and supported on Al_2O_3, which was used as a catalyst for acetylene hydrogenation. It was found that the easier decomposition of subsurface H in Pd(100) facets contributed to its higher activity and the strong adsorption of reactants on Pd(111) facets surface decreased ethylene selectivity.

In this paper, PdNPs stabilized by methyl cellulose (MC) were synthesized in an aqueous solution, which are monodispersed nanoparticles. PdNPs/α-Al_2O_3 catalyst was prepared with monodispersed PdNPs stabilized by MC. Monodispersed PdNPs were spherical or elliptical nanoparticles with exposed (111) and (100) facets. Moreover, the PdNPs/α-Al_2O_3 catalyst showed a more concentrated distribution of Pd particles on the surface of α-Al_2O_3 support than the Pd/α-Al_2O_3 catalyst prepared by the incipient wetness impregnation method using $Pd(NO_3)_2$ as a precursor. The preparation method in this work achieved the highly dispersed PdNPs/α-Al_2O_3 catalyst with smaller Pd particle size and decreased the aggregation of Pd active sites. Therefore, the PdNPs/α-Al_2O_3 catalyst had higher acetylene conversion and ethylene selectivity.

2. Results and Discussion

2.1. Catalyst Characterization

The transmission electron microscopy (TEM) image shown in Figure 1a indicates that the PdNPs stabilized by MC are monodispersed spherical or elliptical nanoparticles. The average particle size is 3.2 nm and the deviation from the mean diameter is about $\pm$0.4 nm. As shown in Figure 1b, the high-resolution TEM (HRTEM) image provides the crystal structure of PdNPs. It shows that PdNPs exposed two kinds of crystal facets, which are attributed to Pd(111) and Pd(100) facets. Moreover, the (111) and (100) lattice fringes in PdNPs exhibited a clearly ordered continuous fringe pattern corresponding to the face-centered cubic (fcc) structure [28]. According to the literature, for the selective hydrogenation of acetylene in ethylene-rich stream, the shape of PdNPs had no impact on ethylene selectivity. Moreover, Pd(111) facets had strong adsorption to the target reactant, and are thus responsible for a higher acetylene conversion than Pd(100) facets [25].

For supported Pd/Al_2O_3 catalysts, isolated Pd active sites dispersed on the surface of the Al_2O_3 support as egg-shell catalysts exhibited high activity for acetylene removal, which also inhibited the over-hydrogenation of ethylene to ethane. Therefore, it is significant to decrease Pd active site ensembles [5,7,11,16]. Figure 2a shows that the PdNPs on the PdNPs/α-Al_2O_3 catalyst were smaller particles than those on the Pd/α-Al_2O_3 catalyst (Figure 2b). This means that the PdNPs/α-Al_2O_3 catalyst prepared with monodispersed PdNPs can achieve highly dispersed active sites. As can be seen in Figure 2c, the PdNPs on the PdNPs/α-Al_2O_3 catalyst are isolated Pd particles, which decrease the Pd ensemble size. In contrast, the Pd particles on the Pd/α-Al_2O_3 catalyst can form large Pd ensembles, which are the aggregation of Pd active sites. Also, the Pd dispersion of the PdNPs/α-Al_2O_3 catalyst was 25.12%. The Pd dispersion of the Pd/α-Al_2O_3 catalyst was 20.36%, which was lower than that of the PdNPs/α-Al_2O_3 catalyst.

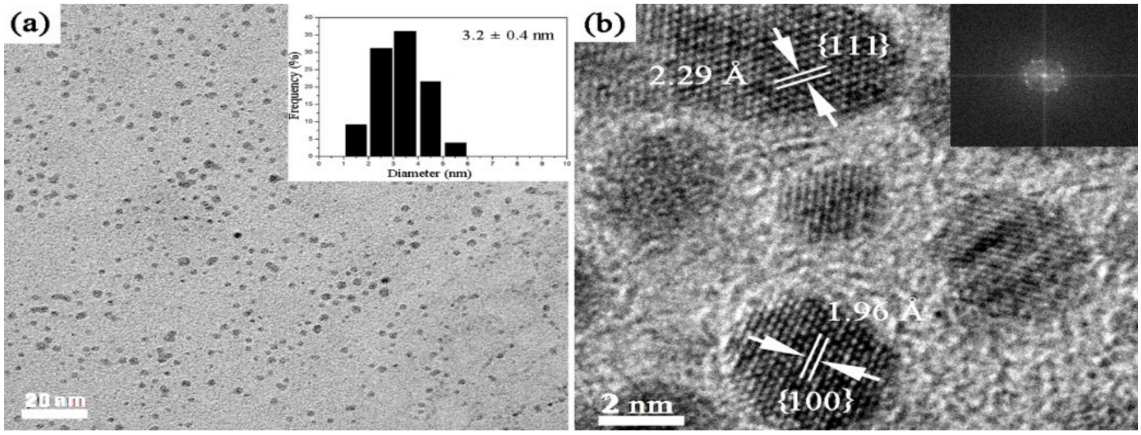

Figure 1. (**a**) TEM image of Pd nanoparticles (PdNPs); the inset is the corresponding Pd particle size distribution; (**b**) HRTEM image of PdNPs; the inset is the corresponding fast Fourier transform image.

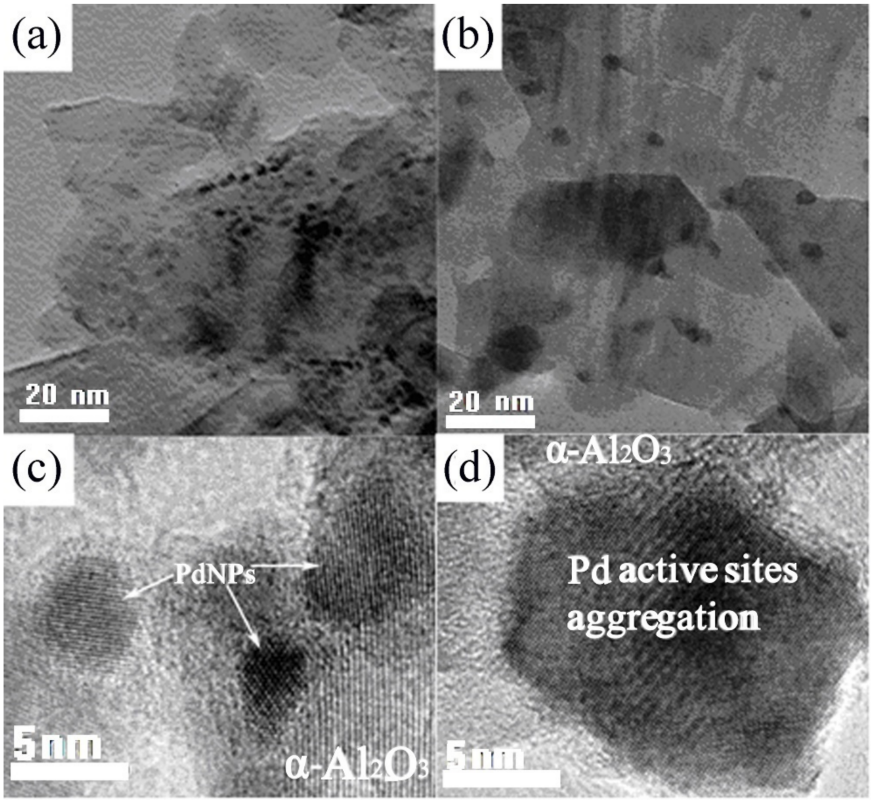

Figure 2. TEM images of (**a**) PdNPs/α-Al_2O_3 catalyst and (**b**) Pd/α-Al_2O_3 catalyst; HRTEM images of (**c**) PdNPs/α-Al_2O_3 catalyst and (**d**) Pd/α-Al_2O_3 catalyst.

To investigate the distribution range of Pd on the α-Al_2O_3 support, SEM images and energy dispersive X-ray spectroscopy (EDS) analysis were taken for the PdNPs/α-Al_2O_3 catalyst and Pd/α-Al_2O_3 catalyst, as shown in Figure 3A. It can be found that the Pd loading on the black rectangular area of the α-Al_2O_3 support was 0.67 wt % by EDS analysis. From surface to centre, the Pd loading on the red and blue rectangular area of the α-Al_2O_3 support was 0.27 wt % and 0.11 wt %, respectively. This indicates that the Pd loading had obviously decreased in the range of 0–200 μm from surface to centre for the PdNPs/α-Al_2O_3 catalyst. As shown in Figure 3B, for the Pd/α-Al_2O_3 catalyst, the Pd loading on the black rectangular area of the α-Al_2O_3 support was

0.40 wt % by EDS analysis. From surface to centre, the Pd loading on the red and blue rectangular area of the α-Al_2O_3 support was 0.19 wt % and 0.13 wt %, respectively. This shows that the Pd loading decreased gradually in the range of 0–1000 μm from surface to centre for the Pd/α-Al_2O_3 catalyst. In this work, the PdNPs/α-Al_2O_3 catalyst showed a more concentrated distribution of Pd particles on the surface of the α-Al_2O_3 support than the Pd/α-Al_2O_3 catalyst. For the selective hydrogenation of acetylene, the catalytic performance of the supported Pd catalysts mainly depends on the dispersion of Pd particles on the α-Al_2O_3 support surface. Although porous oxide supports can provide a large surface area to form egg-shell catalysts, Pd particles dispersed on the long pores might decrease the utilization efficiency of Pd active sites [12,15,16,20,22]. Therefore, it is significant to achieve a more concentrated distribution of Pd particles on the surface of the α-Al_2O_3 support.

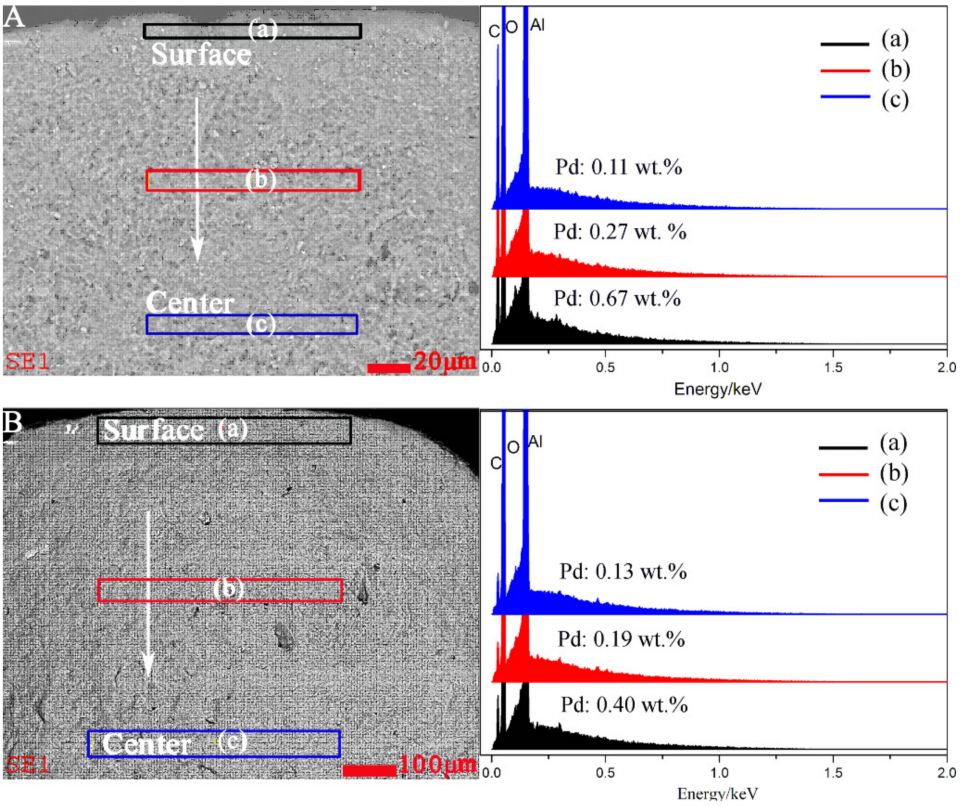

Figure 3. SEM images and energy dispersive X-ray spectroscopy (EDS) spectra of (**A**) PdNPs/α-Al_2O_3 catalyst and (**B**) Pd/α-Al_2O_3 catalyst.

X-ray photoelectron spectroscopy (XPS) analysis was performed to investigate the valence state of the Pd element present in the PdNPs/α-Al_2O_3 catalyst and Pd/α-Al_2O_3 catalyst. As can be seen from Figure 4, the valence state of Pd element was revealed by XPS spectra. The $Pd_{3d5/2}$ peaks of the PdNPs/α-Al_2O_3 and Pd/α-Al_2O_3 catalysts are both at 335.2 eV, which show that the valence states of Pd element in the PdNPs/α-Al_2O_3 and Pd/α-Al_2O_3 catalysts were metallic Pd(0) [29]. In addition, X-ray powder diffraction measurements were also carried out. Figure 5 shows the XRD patterns of the PdNPs/α-Al_2O_3 catalyst and Pd/α-Al_2O_3 catalyst. The characteristic peaks show the strong peaks of α-Al_2O_3 (2θ = 25.57, 35.15, 37.77, 43.35, 52.50, 57.49, 61.30, 66.51, 68.20 and 76.88, the international centre for diffraction data (ICDD) file no.: 82-1468) and the weak peaks of θ-Al_2O_3 (2θ = 31.47, 32.77, 36.68, 38.92, 39.85, 44.83, 47.62, 59.89, 64.02 and 67.41, ICDD file no.: 35-0121). Meanwhile, it should be noted that no typical diffraction peaks of Pd element are detected in the PdNPs/α-Al_2O_3 catalyst and Pd/α-Al_2O_3 catalyst. The reason for this can be attributed to the low weight Pd loading or the small

size of PdNPs on the surface of the PdNPs/α-Al_2O_3 catalyst and Pd/α-Al_2O_3 catalyst. According to the literature, similar phenomena have been reported by Lin et al. [30] and Chen et al. [31].

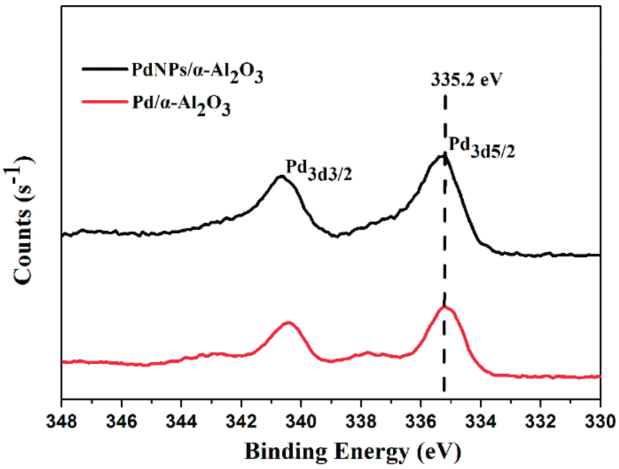

Figure 4. XPS analysis (Pd 3D spectrum) of PdNPs/α-Al_2O_3 catalyst and Pd/α-Al_2O_3 catalyst.

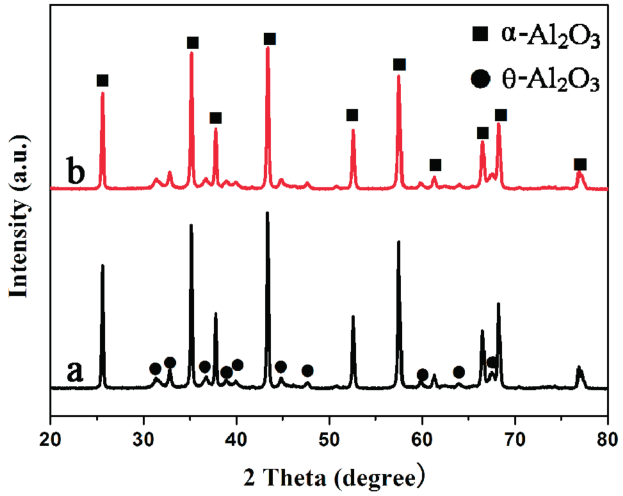

Figure 5. XRD patterns of (**a**) PdNPs/α-Al_2O_3 catalyst and (**b**) Pd/α-Al_2O_3 catalyst.

The real Pd elemental contents of the PdNPs/α-Al_2O_3 catalyst and Pd/α-Al_2O_3 catalyst were analyzed by inductively coupled plasma mass spectrometry (ICP-MS). Table 1 shows the results of the PdNPs/α-Al_2O_3 catalyst and Pd/α-Al_2O_3 catalyst measured by ICP-MS. As can be seen from Table 1, the real values of Pd-loading on the PdNPs/α-Al_2O_3 catalyst and Pd/α-Al_2O_3 catalyst are 0.028 wt % and 0.029 wt %, respectively, which are in accordance with the design values. It also indicated that the PdNPs/α-Al_2O_3 catalyst prepared with monodispersed PdNPs can nearly achieve the same Pd-loading on the α-Al_2O_3 support as the Pd/α-Al_2O_3 catalyst prepared by the incipient wetness impregnation method using $Pd(NO_3)_2$ as a precursor. Moreover, the real values of Pd-loading after 60 h on stream reaction are constant. It is demonstrated that Pd active sites can be firmly attached to the α-Al_2O_3 support by heat treatment. Therefore, the catalysts were usually calcined in air at 450 °C for 4 h during the preparation.

Table 1. The Pd elemental contents of the catalysts (measured by inductively coupled plasma-mass spectrometry (ICP-MS).

Sample	The Design Value of Pd-Loading (wt %)	The Real Value of Pd-Loading before Reaction (wt %)	The Real Value of Pd-Loading after 60 h on Stream Reaction (wt %)
PdNPs/α-Al_2O_3	0.030	0.028	0.028
Pd/α-Al_2O_3	0.030	0.029	0.029

2.2. Catalytic Performance

Figure 6a shows that the catalytic activity of the PdNPs/α-Al_2O_3 catalyst was a little higher than that of the Pd/α-Al_2O_3 catalyst for the selective hydrogenation of acetylene in the temperature range of 50–120 °C. As shown in Figure 6b, the PdNPs/α-Al_2O_3 catalyst also possesses higher ethylene selectivity than that of the Pd/α-Al_2O_3 catalyst at the same reaction condition. Both of these two catalysts present a similar tendency for ethylene selectivity to decrease as acetylene conversion increased, when the reaction temperature increased from 50 to 120 °C. The selective hydrogenation of acetylene in the ethylene-rich stream was a typical consecutive reaction. Ethylene was produced as an intermediate during the reaction. Therefore, ethylene selectivity decreased as acetylene conversion increased [28,32].

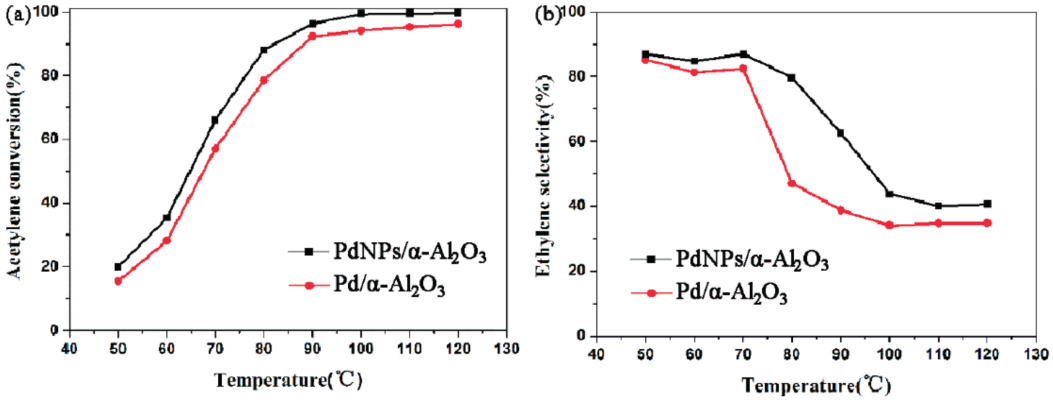

Figure 6. (**a**) Acetylene conversion on PdNPs/α-Al_2O_3 catalyst and Pd/α-Al_2O_3 catalyst; (**b**) Ethylene selectivity on PdNPs/α-Al_2O_3 catalyst and Pd/α-Al_2O_3 catalyst. (Reaction conditions: the ethylene-rich stream containing 0.61% H_2, 0.42% C_2H_2, 7.69% C_2H_6, and balanced C_2H_4 was used for the reaction at atmospheric pressure. Total gas hourly space velocity was 10,000 h^{-1}).

The stabilities of the PdNPs/α-Al_2O_3 catalyst and Pd/α-Al_2O_3 catalyst were tested online by using a microreactor-GC system. As shown in Figure 7, for 60 h on stream, the acetylene conversion of the PdNPs/α-Al_2O_3 catalyst was always kept at 99%, which showed a stable catalytic activity. Its selectivity to ethylene was around 40%. In contrast, the catalytic performance of the Pd/α-Al_2O_3 catalyst was also stable at the beginning of the 24 h. Its acetylene conversion was almost kept at 97% and its selectivity to ethylene was around 34%, which was 6% lower than that of the PdNPs/α-Al_2O_3 catalyst. However, it can be seen that the acetylene conversion of the Pd/α-Al_2O_3 catalyst decreased slightly after 24 h. Meanwhile, ethylene selectivity also increased gradually. It is demonstrated that the catalytic performance of the PdNPs/α-Al_2O_3 catalyst is more stable than the Pd/α-Al_2O_3 catalyst. The excellent catalytic performance may be ascribed to the preparation method in this work, which achieved the highly dispersed PdNPs/α-Al_2O_3 catalyst with a more concentrated distribution of isolated Pd active sites on the surface of the α-Al_2O_3 support.

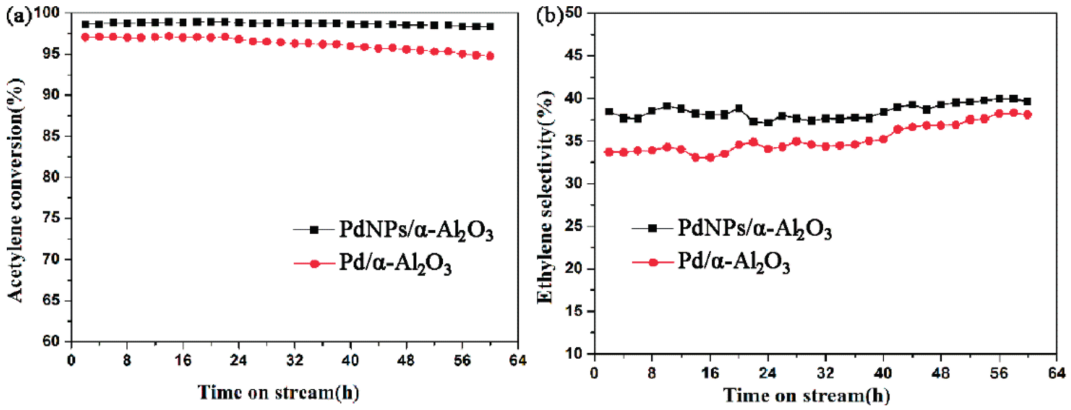

Figure 7. The stabilities of PdNPs/α-Al_2O_3 catalyst and Pd/α-Al_2O_3 catalyst during the reaction with time on stream: (**a**) Acetylene conversion and (**b**) ethylene selectivity. (Reaction conditions: the ethylene-rich stream containing 0.61% H_2, 0.42% C_2H_2, 7.69% C_2H_6, and balanced C_2H_4 was used for the reaction at atmospheric pressure. The reaction temperature was kept at 110 °C. Total gas hourly space velocity was 10,000 h^{-1}).

3. Materials and Methods

3.1. Synthesis

The aqueous solution of $Pd(NO_3)_2$ (1 mg/mL) was obtained from Sinopec Beijing Research Institute of Chemical Industry. Methyl cellulose (average Mw: 40,000) was supplied by Sigma-Aldrich (Saint Louis, MO, USA). In a typical process, a 60-mL aliquot of a 1 mg/mL solution of $Pd(NO_3)_2$ was added to 140 mL of a 0.043 wt % aqueous solution of soluble MC. Meanwhile, the pH was adjusted to about 8.5 by dropwise addition of an aqueous solution of sodium hydroxide (NaOH, 0.5 M). The stirring speed was 300 rpm. The mixture was treated with ultrasonic for 30 min. Then the mixture in a stainless steel autoclave was treated with a gas flow (10% H_2 in Ar) passing through the solution at 40 °C for at least 30 min at atmospheric pressure. The stirring speed was 300 rpm. Finally, monodispersed PdNPs stabilized by MC were synthesized in the aqueous solution.

The support of α-Al_2O_3 consisted of spherical pellets (average diameter 3.5 mm, BET surface area 30.9 m^2/g), which were produced by Sinopec Beijing Research Institute of Chemical Industry. The 200.0 g α-Al_2O_3 support was put in a laboratory coating machine (rotating speed: 100 rpm). Then the above solution of monodispersed PdNPs stabilized by MC was mist-sprayed onto the support using a home-made glass sprayer actuated by compressed air (pressure: 0.1 MPa). Then, the catalyst was dried at 120 °C for 6 h. The catalyst was subsequently calcined in air at 450 °C for 4 h to remove the MC and re-expose the palladium active sites. The obtained catalyst was marked as the PdNPs/α-Al_2O_3 catalyst. For comparison, the Pd/α-Al_2O_3 catalyst (0.03 wt % Pd loading) was prepared by the same method using an aqueous solution of the desired amount of $Pd(NO_3)_2$.

3.2. Characterizations

The catalysts were characterized by transmission electron microscopy (TEM), scanning electron microscopy (SEM), energy dispersive X-ray spectroscopy (EDS), and X-ray photoelectron spectroscopy (XPS). TEM images were recorded by a JEOL JEM-3010 (200 kV) (JEOL, Tokyo, Japan). The SEM observation was performed on FEI XL30 ESEM-FEG (FEI, Eindhoven, The Netherlands) and energy dispersive X-ray analysis was coupled to SEM. X-ray photoelectron spectroscopy (XPS) measurements were measured on a Perkin-Elmer PHI 5600 spectrophotometer (Perkin Elmer Limited, Waltham Mass, Waltham, MA, USA) with the MgK_α radiation. BET surface area was determined by an ASAP 2020C instrument (Micromeritics Instruments, Norcross, GA, USA). Pd dispersion was measured using CO pulse chemisorption by an AutoChem II 2920 instrument (Micromeritics Instruments, Norcross, GA,

USA). XRD analysis was performed on a Bruker AXS D8 Advance instrument (λ = 1.5406 Å; tube voltage, 40 kV; tube current, 300 mA) (Bruker, Karlsruhe, Germany). The ICP analysis was performed by taking a 1.0-g sample into a Teflon crucible, adding 20 mL HNO_3 (BV-III) and leaving one night, followed by ultrasonic treatment for 3 h, and subsequent 50-fold dilution with 2% HNO_3. Finally, this was analyzed with an Agilent 7500CX ICP-MS (Agilent Technologies, Santa Clara, CA, USA).

3.3. Catalytic Tests

For catalytic performance tests, the selective hydrogenation of acetylene in the ethylene-rich stream was performed by using a microreactor-GC system with 1 mL of the catalyst. The microreactor was an 8 mm (i.d.) stainless steel tube. The catalyst was completely immersed in a continuous ethylene-rich gas flow. Before the reaction, the catalyst was reduced by H_2 (gas hourly space velocity: 300 h^{-1}) at 180 °C for 2 h. A feed gas consisting of 0.61% H_2, 0.42% C_2H_2, 7.69% C_2H_6, and balanced with C_2H_4 was used for the reaction. The total gas hourly space velocity (GHSV) was 10,000 h^{-1}. The products were analyzed online by gas chromatography (Agilent 7890, Agilent Technologies, Palo Alto, CA, USA) with FID and TCD detectors. According to the literature, acetylene conversion and ethylene selectivity were calculated by the following equations [32,33]:

$$X_{C_2H_2} = \left[1 - \frac{x_{C_2H_2}}{x^0_{C_2H_2}}\right] \times 100\% \quad (1)$$

$$S_{C_2H_4} = -\frac{\Delta C_2H_4}{\Delta C_2H_2} \times 100\% \quad (2)$$

4. Conclusions

In summary, monodispersed PdNPs stabilized by MC were successfully synthesized in an aqueous solution. The monodispersed PdNPs were supported on an α-Al_2O_3 catalyst to prepare the PdNPs/α-Al_2O_3 catalyst, which had a more concentrated distribution of Pd particles on the surface of the α-Al_2O_3 support. Compared with the Pd/α-Al_2O_3 catalyst, which was prepared by the incipient wetness impregnation method using $Pd(NO_3)_2$ as a precursor, the PdNPs/α-Al_2O_3 catalyst exhibited better catalytic performance for the selective hydrogenation of acetylene. The enhanced catalytic property can be attributed to the preparation method, which can achieve the highly dispersed PdNPs/α-Al_2O_3 catalyst with smaller Pd particle size and decreased the aggregation of Pd active sites.

Acknowledgments: This work was supported by the National Natural Science Foundation of China (51504083, 51404097), Program for Science & Technology Innovation Talents in Universities of Henan Province (17HASTIT029), the Research Foundation for Youth Scholars of Higher Education of Henan Province (2016GGJS-040), Natural Science Foundation of Henan Province of China (162300410113), Program for Innovative Research Team (in Science and Technology) in the University of Henan Province (16IRTSTHN005), Education Department Natural Science Foundation of Henan Province (17A430019), the Fundamental Research Funds for the Universities of Henan Province (NSFRF1606, NSFRF140101) and Foundation for Distinguished Young Scientists of Henan Polytechnic University (J2016-2, J2017-3).

Author Contributions: Huoli Zhang and Qingjie Tang designed and performed the experiments; Peng Kang provided the characterization of the catalyst samples; Yan Wang and Mingjie Ma analyzed the data; Youchao Wang and Jianliang Cao provided the idea of this work and managed all the experimental and writing process as the corresponding authors.

Conflicts of Interest: The authors declare no conflict of interest.

References

1. Borodziński, A.; Bond, G.C. Selective hydrogenation of ethyne in ethane-rich streams on palladium catalysts, Part 1: Effect of changes to the catalyst during reaction. *Catal. Rev.* **2006**, *48*, 91–144. [CrossRef]
2. Borodziński, A.; Bond, G.C. Selective hydrogenation of ethyne in ethene-rich streams on palladium catalysts, Part 2: Steady-state kinetics and effects of palladium particle size, carbon monoxide, and promoters. *Catal. Rev.* **2008**, *50*, 379–469. [CrossRef]

3. Árpád, M.; Sárkány, A.; Varga, M. Hydrogenation of carbon-carbon multiple bonds: Chemo-, regio- and stereo-selectivity. *J. Mol. Catal. A: Chem.* **2001**, *173*, 185–221.
4. Yang, B.; Burch, R.; Hardacre, C.; Hu, P.; Hughes, P. Importance of surface carbide formation on the activity and selectivity of Pd surfaces in the selective hydrogenation of acetylene. *Surf. Sci.* **2016**, *646*, 45–49. [CrossRef]
5. Zhang, H.; Cao, J.; Wu, B.; Dai, W.; Chen, Z.; Ma, M. An alumina-coated, egg-shell Pd/α-Al_2O_3@SiC catalyst with enhanced ethylene selectivity in the selective hydrogenation of acetylene. *RSC Adv.* **2016**, *6*, 57174–57182. [CrossRef]
6. Ravanchi, M.T.; Sahebdelfar, S. Pd-Ag/Al_2O_3 catalyst: Stages of deactivation in tail-end acetylene selective hydrogenation. *Appl. Catal. A: Gen.* **2016**, *525*, 197–203. [CrossRef]
7. Ravanchi, M.T.; Sahebdelfar, S.; Fard, M.R.; Fadaeerayeni, S.; Bigdeli, P. Pd-Ag/α-Al_2O_3 Catalyst Deactivation in Acetylene Selective Hydrogenation Process. *Chem. Eng. Technol.* **2016**, *39*, 301–310. [CrossRef]
8. He, Y.; Liang, L.; Liu, Y.; Feng, J.; Ma, C.; Li, D. Partial hydrogenation of acetylene using highly stable dispersed bimetallic Pd–Ga/MgO–Al_2O_3 catalyst. *J. Catal.* **2014**, *309*, 166–173. [CrossRef]
9. McCue, A.J.; McRitchie, C.J.; Shepherd, A.M.; Anderson, J.A. Cu/Al_2O_3 catalysts modified with Pd for selective acetylene hydrogenation. *J. Catal.* **2014**, *319*, 127–135. [CrossRef]
10. Zhu, B.; Jang, B.W.L. Insights into surface properties of non-thermal RF plasmas treated Pd/TiO_2 in acetylene hydrogenation. *J. Mol. Catal. A: Chem.* **2014**, *395*, 137–144. [CrossRef]
11. Pei, G.X.; Liu, X.Y.; Wang, A.; Lee, A.F.; Isaacs, M.A.; Li, L.; Pan, X.; Yang, X.; Wang, X.; Tai, Z.; et al. Ag alloyed Pd single-atom catalysts for efficient selective hydrogenation of acetylene to ethylene in excess ethylene. *ACS Catal.* **2015**, *5*, 3717–3725. [CrossRef]
12. Zhang, Y.; Diao, W.; Williams, C.T.; Monnier, J.R. Selective hydrogenation of acetylene in excess ethylene using Ag-and Au–Pd/SiO_2 bimetallic catalysts prepared by electroless deposition. *Appl. Catal. A: Gen.* **2014**, *469*, 419–426. [CrossRef]
13. Menezes, W.G.; Altmann, L.; Zielasek, V.; Thiel, K.; Bäumer, M. Bimetallic Co–Pd catalysts: Study of preparation methods and their influence on the selective hydrogenation of acetylene. *J. Catal.* **2013**, *300*, 125–135. [CrossRef]
14. Zhang, S.; Chen, C.Y.; Jang, B.W.L.; Zhu, A.M. Radio-frequency H_2 plasma treatment of AuPd/TiO_2 catalyst for selective hydrogenation of acetylene in excess ethylene. *Catal. Today* **2015**, *256*, 161–169. [CrossRef]
15. Zhang, Y.; Diao, W.; Monnier, J.R.; Williams, C.T. Pd–Ag/SiO_2 bimetallic catalysts prepared by galvanic displacement for selective hydrogenation of acetylene in excess ethylene. *Catal. Sci. Technol.* **2015**, *5*, 4123–4132. [CrossRef]
16. Kuhn, M.; Lucas, M.; Claus, P. Long-Time Stability vs. Deactivation of Pd–Ag/Al_2O_3 Egg-Shell Catalysts in Selective Hydrogenation of Acetylene. *Ind. Eng. Chem. Res.* **2015**, *54*, 6683–6691. [CrossRef]
17. Komeili, S.; Ravanchi, M.T.; Taeb, A. The influence of alumina phases on the performance of the Pd–Ag/Al_2O_3 catalyst in tail-end selective hydrogenation of acetylene. *Appl. Catal. A: Gen.* **2015**, *502*, 287–296. [CrossRef]
18. Riyapan, S.; Zhang, Y.; Wongkaew, A.; Pongthawornsakun, B.; Monnier, J.R.; Panpranot, J. Preparation of improved Ag–Pd/TiO_2 catalysts using the combined strong electrostatic adsorption and electroless deposition methods for the selective hydrogenation of acetylene. *Catal. Sci. Technol.* **2016**, *6*, 5608–5617. [CrossRef]
19. Jin, Q.; He, Y.; Miao, M.; Guan, C.; Du, Y.; Feng, J.; Li, D. Highly selective and stable PdNi catalyst derived from layered double hydroxides for partial hydrogenation of acetylene. *Appl. Catal. A: Gen.* **2015**, *500*, 3–11. [CrossRef]
20. Liu, J.H.; Meng, L.D.; Lv, C.Q.; Wang, G.C. Selective hydrogenation of acetylene over TiO_2-supported PdAg cluster: Carbon species effect. *RSC Adv.* **2016**, *6*, 14593–14601. [CrossRef]
21. Krajčí, M.; Hafner, J. Selective semi-hydrogenation of acetylene: Atomistic scenario for reactions on the polar threefold surfaces of GaPd. *J. Catal.* **2014**, *312*, 232–248. [CrossRef]
22. Han, Y.; Peng, D.; Xu, Z.; Wan, H.; Zheng, S.; Zhu, D. TiO_2 supported Pd@Ag as highly selective catalysts for hydrogenation of acetylene in excess ethylene. *Chem. Commun.* **2013**, *49*, 8350–8352. [CrossRef] [PubMed]
23. Yarulin, A.E.; Crespo-Quesada, R.M.; Egorova, E.V.; Kiwi-Minsker, L.L. Structure sensitivity of selective acetylene hydrogenation over the catalysts with shape-controlled palladium nanoparticles. *Kinet. Catal.* **2012**, *53*, 253–261. [CrossRef]

24. Shokouhimehr, M.; Shin, K.Y.; Lee, J.S.; Hackett, M.J.; Jun, S.W.; Oh, M.H.; Jang, J.; Hyeon, T. Magnetically recyclable core–shell nanocatalysts for efficient heterogeneous oxidation of alcohols. *J. Mater. Chem. A* **2014**, *2*, 7593–7599. [CrossRef]
25. Shokouhimehr, M. Magnetically separable and sustainable nanostructured catalysts for heterogeneous reduction of nitroaromatics. *Catalysts* **2015**, *5*, 534–560. [CrossRef]
26. Crespo-Quesada, M.; Andanson, J.M.; Yarulin, A.; Lim, B.; Xia, Y.; Kiwi-Minsker, L. UV–ozone cleaning of supported poly (vinylpyrrolidone)-stabilized palladium nanocubes: Effect of stabilizer removal on morphology and catalytic behavior. *Langmuir* **2011**, *27*, 7909–7916. [CrossRef] [PubMed]
27. He, Y.F.; Feng, J.T.; Du, Y.Y.; Li, D.Q. Controllable synthesis and acetylene hydrogenation performance of supported Pd nanowire and cuboctahedron catalysts. *ACS Catal.* **2012**, *2*, 1703–1710. [CrossRef]
28. Kim, S.K.; Kim, C.; Lee, J.H.; Kim, J.; Lee, H.; Moon, S.H. Performance of shape-controlled Pd nanoparticles in the selective hydrogenation of acetylene. *J. Catal.* **2013**, *306*, 146–154. [CrossRef]
29. Yu, H.; Mao, Z.; Dai, W.; Peng, J.; Zhai, M.; Wei, G. Highly selective Pd/Al_2O_3 catalyst for hydrogenation of methylacetylene and propadiene in propylene stream prepared by γ-radiation. *Appl. Catal. A: Gen.* **2012**, *445*, 246–251. [CrossRef]
30. Lin, X.; Xu, D.; Xi, Y.; Zhao, R.; Zhao, L.; Song, M.; Zhai, H.; Che, G.; Chang, L. Construction of leaf-like $g\text{-}C_3N_4/Ag/BiVO_4$ nanoheterostructures with enhanced photocatalysis performance under visible-light irradiation. *Colloids Surf. A: Physicochem. Eng. Asp.* **2017**, *513*, 117–124. [CrossRef]
31. Chen, Y.; Huang, W.; He, D.; Situ, Y.; Huang, H. Construction of heterostructured $g\text{-}C_3N_4/Ag/TiO_2$ microspheres with enhanced photocatalysis performance under visible-light irradiation. *ACS Appl. Mater. Interfaces* **2014**, *6*, 14405–14414. [CrossRef] [PubMed]
32. Kang, J.H.; Shin, E.W.; Kim, W.J.; Park, J.D.; Moon, S.H. Selective hydrogenation of acetylene on TiO_2-added Pd catalysts. *J. Catal.* **2002**, *208*, 310–320. [CrossRef]
33. Pachulski, A.; Schödel, R.; Claus, P. Performance and regeneration studies of $Pd\text{-}Ag/Al_2O_3$ catalysts for the selective hydrogenation of acetylene. *Appl. Catal. A: Gen.* **2011**, *400*, 14–24. [CrossRef]